Appl. Math. Mech. -Engl. Ed., **33**(5), 631–648 (2012)
DOI 10.1007/s10483-012-1576-6

Applied Mathematics and Mechanics (English Edition)

MHD stagnation point flow towards heated shrinking surface subjected to heat generation/absorption*

T. HAYAT[1,2], M. HUSSAIN[1], A. A. HENDI[2], S. NADEEM[1]

(1. Department of Mathematics, Quaid-i-Azam University, Islamabad 44000, Pakistan;
2. Department of Physics, Faculty of Science, King Saud University,
Riyadh 11321, Saudi Arabia)

Abstract The magnetohydrodynamic (MHD) stagnation point flow of micropolar fluids towards a heated shrinking surface is analyzed. The effects of viscous dissipation and internal heat generation/absorption are taken into account. Two explicit cases, i.e., the prescribed surface temperature (PST) and the prescribed heat flux (PHF), are discussed. The boundary layer flow and energy equations are solved by employing the homotopy analysis method. The quantities of physical interest are examined through the presentation of plots/tabulated values. It is noticed that the existence of the solutions for high shrinking parameters is associated closely with the applied magnetic field.

Key words stagnation point flow, micropolar fluid, shrinking sheet, convergence, homotopy analysis method

Chinese Library Classification O361.3
2010 Mathematics Subject Classification 76W05

1 Introduction

The interest in the study of flows induced by a moving surface in otherwise quiescent fluids has grown considerably during the last few decades. This type of flows has a special relevance in the manufacturing process including glass fiber drawing, crystal growing, etc. Such systems in the presence of heat transfer have practical applications in extrusion process and continuous casting. In view of such motivation, there are many extensive researches on this topic. Mahapatra and Gupta[1] studied the stagnation point flow towards a stretching surface in the presence of an applied magnetic field. Nazar et al.[2] addressed the unsteady boundary layer flow in the region of the stagnation point over a stretching surface. Lok et al.[3] investigated the unsteady mixed convection flow of a micropolar fluid near the stagnation point on a vertical surface. Lok et al.[4] studied the mixed convection flow over a non-orthogonal stagnation point towards a stretching vertical plate. They considered both assisting and opposing flows, and found that the flow had an inverted boundary layer suction when the stretching velocity of the surface exceeded the stagnation velocity of the free stream. Wang[5] examined the stagnation flow towards a rotating disk and a shrinking sheet. Xu et al.[6] discussed the series solutions of the unsteady boundary layer flow of a micropolar fluid near the forward stagnation point of a plane surface, and compared the results with an exact solution. Nadeem et al.[7] extended the idea

* Received Dec. 3, 2010 / Revised Dec. 29, 2011
Project supported by the Higher Education Commission (HEC) of Pakistan (No. 106-1396-Ps6-004)
Corresponding author M. HUSSAIN, Professor, Ph. D., E-mail: majid_gul@yahoo.com

of Xu et al.[6] and discussed the magnetohydrodynamic (MHD) stagnation flow of a micropolar fluid through a porous medium. Kumari and Nath[8] examined the steady mixed convection stagnation-point flow of an upper convected Maxwell fluid with a magnetic field. Hayat et al.[9] discussed the MHD stagnation-point flow of an upper-convected Maxwell fluid over a stretching surface. Recently, Labropulu et al.[10] studied the non-orthogonal stagnation-point flow towards a stretching surface in a non-Newtonian fluid with heat transfer. It is noticed that the majority of the boundary layer flows are addressed for the stretching surface in the presence/absence of stagnation point flows. Very little information is available on the flows caused by the shrinking surface (see Refs. [11–15]).

On the other hand, micropolar fluids are quite popular among the researchers recently. Such fluids consist of dumbel shaped molecules or short rigid cylindrical elements, polymer fluids with suspension, etc. The dust or smoke in a gas can be easily described by the dynamics of micropolar fluids. In fact, the theory of micropolar fluids has been proposed by Eringen[16–17]. Using this theory, many other researchers have discussed the micropolar fluids with different geometries and flow problems. Devakar and Iyengar[18] studied Stokes' first problem for a micropolar fluid through a state-space approach. Ali and Hayat[19] studied the peristaltic flow of a micropolar fluid in an asymmetric channel. More recently, Magyari and Kumaran[20] examined the generalized Crane flow of micropolar fluids. Ariman et al.[21] presented an excellent review of micropolar fluids and related applications. Utilizing the theory of micropolar fluids, it is experimentally shown by Hoyt and Fabula[22] that the skin friction is reduced by $25\% - 30\%$ when the fluids containing minute polymeric additions are considered. Power[23] pointed out that the dynamics of body fluids, e.g., the fluid in the brain, can be described by using a micropolar fluid model.

The aim of the current article is to address the stagnation flow and heat transfer in a micropolar fluid over a shrinking surface. The fluid is electrically conducting in the presence of a constant magnetic field applied in the transverse direction to the flow. Two cases, i.e., the prescribed surface temperature (PST) and the prescribed heat flux (PHF), are examined. The energy equation includes the viscous dissipation. The homotopy analysis method is employed for the series solutions of the governing problems. This technique has been successfully utilized in some recent studies[24–34]. Finally, the effects of the embedded parameters on the velocity, temperature, skin friction, and Nusselt number are analyzed.

2 Governing equations and boundary conditions

We investigate the stagnation point flow of an incompressible electrically conducting micropolar fluid towards a porous shrinking sheet. A magnetic field with the constant strength B_0 is exerted transversely to the sheet. The electric field is not considered, and the induced magnetic field effects are negligible, subjected to the assumption of small magnetic Reynolds numbers. The shrinking sheet is at $y = 0$. The boundary layer flow and heat transfer are governed by the following expressions:

$$\frac{\partial u}{\partial x} + \frac{\partial v}{\partial y} = 0, \tag{1}$$

$$u\frac{\partial u}{\partial x} + v\frac{\partial u}{\partial y} = u_{\mathrm{e}}\frac{\mathrm{d}u_{\mathrm{e}}}{\mathrm{d}x} + \left(\nu + \frac{k}{\rho}\right)\frac{\partial^2 u}{\partial y^2} + \frac{k}{\rho}\frac{\partial N}{\partial y} - \frac{\sigma B_0^2}{\rho}(u - u_{\mathrm{e}}), \tag{2}$$

$$u\frac{\partial N}{\partial x} + v\frac{\partial N}{\partial y} = \frac{\gamma}{\rho j}\frac{\partial^2 N}{\partial y^2} - \frac{k}{\rho j}\Big(2N + \frac{\partial u}{\partial y}\Big), \tag{3}$$

$$\rho c_p\Big(u\frac{\partial T}{\partial x} + v\frac{\partial T}{\partial y}\Big) = K^*\frac{\partial^2 T}{\partial y^2} + \mu\Big(\frac{\partial u}{\partial y}\Big)^2 + q(T - T_\infty) \tag{4}$$

subjected to the conditions

$$u = -bx, \quad v = -v_0, \quad N = -n\frac{\partial u}{\partial y}, \quad y = 0, \tag{5}$$

$$u \to u_{\mathrm{e}}(x) = ax, \quad N \to 0, \quad y \to \infty, \tag{6}$$

$$T = T_{\mathrm{w}} = T_\infty + A\Big(\frac{x}{l}\Big)^2 \quad \text{at} \quad y = 0 \quad \text{for the PST case}, \tag{7}$$

$$q_{\mathrm{w}} = -k^*\frac{\partial T}{\partial y} = D\Big(\frac{x}{l}\Big)^2 \quad \text{at} \quad y = 0 \quad \text{for the PHF case}, \tag{8}$$

$$T \to T_\infty, \quad y \to \infty. \tag{9}$$

In the above equations, A and D are the constants, l is the characteristic length, q_{w} is the wall heat flux, u and v are the velocity components along the x- and y-axes, u_{e} $(= ax)$ is the free stream velocity, N is the microrotation velocity, ν is the kinematic viscosity, ρ is the density, n is a constant, both a and b are positive constants, and j, γ, and k are the constant microinertia per unit mass, spin gradient viscosity, and vortex viscosity, respectively. Note that[35]

$$\gamma = \Big(\frac{\mu + k}{2}\Big)j^*, \tag{10}$$

where $j^* = v/b$ is a reference length.

We define the following variables:

$$\begin{cases} u = \dfrac{\partial \Psi}{\partial y} = bxf'(\eta), \\ v = -\dfrac{\partial \Psi}{\partial x} = -(b\nu)^{\frac{1}{2}}f(\eta), \\ N = \Big(\dfrac{b^3}{\nu}\Big)^{\frac{1}{2}}xg(\eta), \\ \eta = \Big(\dfrac{b}{\nu}\Big)^{\frac{1}{2}}y, \quad \Psi = (b\upsilon)^{\frac{1}{2}}xf(\eta), \end{cases} \tag{11}$$

where the prime denotes the derivative with respect to η, and Eq. (1) is automatically satisfied through this choice of stream functions. Further, Eqs. (2)–(3), (5)–(6), and (11) give

$$(1 + K)f''' + ff'' - f'^2 + Kg' - M(f' - 1) + \lambda^2 = 0, \tag{12}$$

$$\Big(1 + \frac{K}{2}\Big)g'' + fg' - f'g - K(2g + f'') = 0, \tag{13}$$

$$f(0) = R, \quad f'(0) = -1, \quad g(0) = -nf''(0), \tag{14}$$

$$f'(\eta) = \lambda, \quad g(\eta) = 0, \quad \eta \to \infty, \tag{15}$$

where $K = k/\mu$ is the microinertia parameter, $M = \sigma B_0^2/(\rho a)$ is the magnetic field parameter, $R = v_0/(b\nu)^{\frac{1}{2}}$ is the porosity parameter, $\lambda = a/b$ (> 0), and the constant $n \in [0, 1]$. Here, $n = 0$ corresponds to the strong concentration of microelements, and $n = \frac{1}{2}$ corresponds to the weak concentration of the particles. The expressions of velocity components depend upon Ψ. They are physical quantities that will be examined in detail in the discussion section.

The dimensionless shear stress and Nusselt number are

$$C_{\mathrm{f}}Re_x^{\frac{1}{2}} = (1 + K)f''(0) + Kg(0), \tag{16}$$

$$Nu_xRe_x^{-\frac{1}{2}} = -\theta'(0). \tag{17}$$

For the PST case, we define

$$\theta(\eta) = \frac{T - T_\infty}{T_\mathrm{w} - T_\infty}. \tag{18}$$

Thus, the relevant problem is

$$\theta'' + Prf\theta' - Pr(2f' - \alpha)\theta = -PrEcf''^2, \tag{19}$$

$$\begin{cases} \theta = 1, & \eta = 0, \\ \theta \to 0, & \eta \to \infty, \end{cases} \tag{20}$$

where Pr is the Prandtl number, α is the internal heat parameter, and Ec is the Eckert number,

$$Pr = \frac{\mu c_p}{K^*}, \quad \alpha = \frac{q}{b}\rho c_p, \quad Ec = \frac{b^2 l^2}{Ac_p}.$$

Considering the PHF case, we set

$$T - T_\infty = \frac{D}{k}\Big(\frac{x}{l}\Big)^2 \Big(\frac{v}{b}\Big)^{\frac{1}{2}} h(\eta). \tag{21}$$

Then, the resulting problem is

$$h'' + Prfh' - Pr(2f' - \alpha)h = -PrEcf''^2, \tag{22}$$

$$\begin{cases} h'(\eta) = -1, & \eta = 0, \\ h \to 0, & \eta \to \infty. \end{cases} \tag{23}$$

Here, Ec is the Eckert number,

$$Ec = \frac{K^* b^2 l^2}{Dc_p}\Big(\frac{b}{v}\Big)^{\frac{1}{2}}.$$

3 Homotopy analysis solutions

The series solutions to $f(\eta)$, $g(\eta)$, $\theta(\eta)$, and $h(\eta)$ in terms of a set of base functions

$$\{\eta^q \exp(-n\eta) | q \geqslant 0,\ n \geqslant 0\} \tag{24}$$

are

$$f(\eta) = A^0_{0,\,0} + \sum_{n=1}^{\infty}\sum_{q=1}^{\infty} A^k_{m,\,n}\eta^{2q}\exp(-n\eta), \tag{25}$$

$$g(\eta) = \sum_{n=0}^{\infty}\sum_{q=0}^{\infty} B^k_{m,\,n}\eta^{q}\exp(-n\eta), \tag{26}$$

$$\theta(\eta) = \sum_{n=0}^{\infty}\sum_{q=0}^{\infty} C^k_{m,\,n}\eta^{q}\exp(-n\eta), \tag{27}$$

$$h(\eta) = \sum_{n=0}^{\infty}\sum_{q=0}^{\infty} D^k_{m,\,n}\eta^{q}\exp(-n\eta), \tag{28}$$

where $A^k_{m,n}$, $B^k_{m,n}$, $C^k_{m,n}$, and $D^k_{m,n}$ are the coefficients. By rule of the solution expression, the initial guesses (f_0, g_0, θ_0, h_0) and the auxiliary linear operators (L_f, L_g, L_θ, L_h) are

$$f_0(\eta) = R + \lambda\eta + (\lambda+1)(\exp(-\eta) - 1), \tag{29}$$

$$g_0(\eta) = -N f_0''(0)\exp(-\eta), \tag{30}$$

$$\theta_0(\eta) = \exp(-\eta), \tag{31}$$

$$h_0(\eta) = \exp(-\eta), \tag{32}$$

$$L_f = \frac{\mathrm{d}^3 f}{\mathrm{d}\eta^3} - \frac{\mathrm{d}f}{\mathrm{d}\eta}, \tag{33}$$

$$L_g = \frac{\mathrm{d}^2 g}{\mathrm{d}\eta^2} - g, \tag{34}$$

$$L_\theta = \frac{\mathrm{d}^2 \theta}{\mathrm{d}\eta^2} - \theta, \tag{35}$$

$$L_h = \frac{\mathrm{d}^2 h}{\mathrm{d}\eta^2} - h, \tag{36}$$

$$L_f(C_1 + C_2\exp\eta + C_3\exp(-\eta)) = 0, \tag{37}$$

$$L_g(C_4\exp\eta + C_5\exp(-\eta)) = 0, \tag{38}$$

$$L_\theta(C_6\exp\eta + C_7\exp(-\eta)) = 0, \tag{39}$$

$$L_h(C_8\exp\eta + C_9\exp(-\eta)) = 0, \tag{40}$$

where C_i ($i = 1, 2, \cdots, 9$) are the arbitrary constants.

Indicate $p \in [0, 1]$ as an embedding parameter and ($\hbar_f$, $\hbar_g$, $\hbar_\theta$, and $\hbar_h$) as the nonzero auxiliary parameters. Then, the zeroth-order problems can be defined by

$$(1-p)L_f(\hat{f}(\eta;\, p) - f_0(\eta)) = p\hbar_f N_f(\hat{f}(\eta;\, p)), \tag{41}$$

$$(1-p)L_g(\hat{g}(\eta;\, p) - g_0(\eta)) = p\hbar_g N_g(\hat{f}(\eta;\, p),\, \hat{g}(\eta;\, p)), \tag{42}$$

$$(1-p)L_\theta(\hat{\theta}(\eta;\, p) - \theta_0(\eta)) = p\hbar_\theta N_\theta(\hat{f}(\eta;\, p),\, \hat{\theta}(\eta;\, p)), \tag{43}$$

$$(1-p)L_h(\hat{h}(\eta;\, p) - h_0(\eta)) = p\hbar_h N_h(\hat{f}(\eta;\, p),\, \hat{h}(\eta;\, p)), \tag{44}$$

$$\begin{cases} \hat{f}(\eta)\Big|_{\eta=0} = R, \quad \dfrac{\partial \hat{f}(\eta)}{\partial\eta}\Big|_{\eta=0} = -1, \\ \hat{g}(\eta)\Big|_{\eta=0} = -N_0\dfrac{\partial^2 \hat{f}(\eta)}{\partial\eta^2}\Big|_{\eta=0}, \quad \hat{\theta}(\eta)\Big|_{\eta=0} = 1, \\ \dfrac{\partial \hat{h}(\eta)}{\partial\eta}\Big|_{\eta=0} = -1, \quad \hat{\theta}(\eta)\Big|_{\eta=\infty} = 0, \\ \hat{g}(\eta)\Big|_{\eta=\infty} = 0, \quad \dfrac{\partial \hat{f}(\eta)}{\partial\eta}\Big|_{\eta=\infty} = \lambda, \quad \hat{h}(\eta)\Big|_{\eta=\infty} = 0, \end{cases} \tag{45}$$

$$\begin{aligned} N_f(\hat{f}(\eta;\, p),\, \hat{g}(\eta;\, p)) = {} & (1+K)\frac{\partial^3 \hat{f}(\eta;\, p)}{\partial\eta^3} + \hat{f}(\eta;\, p)\frac{\partial^2 \hat{f}(\eta;\, p)}{\partial\eta^2} - \Big(\frac{\partial \hat{f}(\eta;\, p)}{\partial\eta}\Big)^2 \\ & + K\frac{\partial \hat{g}(\eta;\, p)}{\partial\eta} - M\frac{\partial \hat{f}(\eta;\, p)}{\partial\eta} + M + \lambda^2, \end{aligned} \tag{46}$$

$$N_g(\hat{f}(\eta;\, p), \hat{g}(\eta;\, p)) = \Big(1+\frac{k}{2}\Big)\frac{\partial^2 \hat{g}(\eta;\, p)}{\partial \eta^2} + \hat{f}(\eta;\, p)\frac{\partial \hat{g}(\eta;\, p)}{\partial \eta} - \hat{f}(\xi, \eta;\, p)\frac{\partial \hat{g}(\eta;\, p)}{\partial \eta} - 2k\hat{g}(\eta;\, p) - k\frac{\partial^2 \hat{f}(\eta;\, p)}{\partial \eta^2}, \tag{47}$$

$$N_\theta(\hat{f}(\eta;\, p),\, \hat{\theta}(\eta;\, p)) = \frac{\partial^2 \hat{\theta}(\eta;\, p)}{\partial \eta^2} + Pr\hat{f}(\eta;\, p)\frac{\partial \hat{\theta}(\eta;\, p)}{\partial \eta} - 2Pr\frac{\partial \hat{f}(\eta;\, p)}{\partial \eta}\hat{\theta}(\eta;\, p) + Pr\alpha\frac{\partial \hat{f}(\eta;\, p)}{\partial \eta}\hat{\theta}(\eta;\, p) + PrEc\Big(\frac{\partial^2 \hat{f}(\eta;\, p)}{\partial \eta^2}\Big)^2, \tag{48}$$

$$N_h(\hat{f}(\eta;\, p),\, \hat{h}(\eta;\, p)) = \frac{\partial^2 \hat{h}(\eta;\, p)}{\partial \eta^2} + Pr\hat{f}(\eta;\, p)\frac{\partial \hat{h}(\eta;\, p)}{\partial \eta} - 2Pr\hat{h}(\eta;\, p)\frac{\partial \hat{f}(\eta;\, p)}{\partial \eta} + Pr\alpha\hat{h}(\eta;\, p) + PrEc\Big(\frac{\partial^2 \hat{f}(\eta;\, p)}{\partial \eta^2}\Big)^2. \tag{49}$$

When $p = 0$ and $p = 1$, we obtain

$$\hat{f}(\eta;\, 0) = f_0(\eta), \quad \hat{f}(\eta;\, 1) = f(\eta), \tag{50}$$

$$\hat{g}(\eta;\, 0) = g_0(\eta), \quad \hat{g}(\eta;\, 1) = g(\eta), \tag{51}$$

$$\hat{\theta}(\eta;\, 0) = \theta_0(\eta), \quad \hat{\theta}(\eta;\, 1) = \theta(\eta), \tag{52}$$

$$\hat{h}(\eta;\, 0) = h_0(\eta), \quad \hat{h}(\eta;\, 1) = h(\eta), \tag{53}$$

$$\hat{f}(\eta;\, p) = f_0(\eta) + \sum_{m=1}^{\infty} f_m(\eta)p^m, \tag{54}$$

$$\hat{g}(\eta;\, p) = g_0(\eta) + \sum_{m=1}^{\infty} g_m(\eta)p^m, \tag{55}$$

$$\hat{\theta}(\eta;\, p) = \theta_0(\eta) + \sum_{m=1}^{\infty} \theta_m(\eta)p^m, \tag{56}$$

$$\hat{h}(\eta;\, p) = h_0(\eta) + \sum_{m=1}^{\infty} h_m(\eta)p^m, \tag{57}$$

$$\begin{cases} f_m(\eta) = \dfrac{1}{m!}\dfrac{\partial^m f(\eta;\, p)}{\partial \eta^m}\Big|_{p=0}, \quad g_m(\eta) = \dfrac{1}{m!}\dfrac{\partial^m g(\eta;\, p)}{\partial \eta^m}\Big|_{p=0}, \\ \theta_m(\eta) = \dfrac{1}{m!}\dfrac{\partial^m \theta(\eta;\, p)}{\partial \eta^m}\Big|_{p=0}, \quad h_m(\eta) = \dfrac{1}{m!}\dfrac{\partial^m h(\eta;\, p)}{\partial \eta^m}\Big|_{p=0}. \end{cases} \tag{58}$$

The values of $\hbar_f$, $\hbar_g$, $\hbar_\theta$, and $\hbar_h$ are selected in such a way that the series solutions are convergent at $p = 1$. Therefore, we have

$$f(\eta) = f_0(\eta) + \sum_{m=1}^{\infty} f_m(\eta), \tag{59}$$

$$g(\eta) = g_0(\eta) + \sum_{m=1}^{\infty} g_m(\eta), \tag{60}$$

$$\theta(\eta) = \theta_0(\eta) + \sum_{m=1}^{\infty} \theta_m(\eta), \tag{61}$$

$$h(\eta) = h_0(\eta) + \sum_{m=1}^{\infty} h_m(\eta). \tag{62}$$

The problems at the mth-order deformation are

$$L_f(f_m(\eta) - \chi_m f_{m-1}(\eta)) = \hbar_f R_m^f(\eta), \tag{63}$$

$$L_g(g_m(\eta) - \chi_m g_{m-1}(\eta)) = \hbar_g R_m^g(\eta), \tag{64}$$

$$L_\theta(\theta_m(\eta) - \chi_m \theta_{m-1}(\eta)) = \hbar_\theta R_m^\theta(\eta), \tag{65}$$

$$L_h(h_m(\eta) - \chi_m h_{m-1}(\eta)) = \hbar_h R_m^h(\eta), \tag{66}$$

$$\begin{cases} f_m(0) = 0, \quad f'_m(0) = 0, \quad f'_m(\infty) = 0, \\ g_m(0) = 0, \quad g_m(\infty) = 0, \quad g'_m(\infty) = 0, \\ \theta_m(0) = 0, \quad \theta_m(\infty) = 0, \\ h'_m(0) = 0, \quad h'_m(\infty) = 0, \end{cases} \tag{67}$$

$$\begin{aligned} R_m^f(\eta) = {} & (1+K) f'''_{m-1} + \sum_{k=0}^{m-1} (f_k f''_{m-1-k} - f'_k f'_{m-1-k}) \\ & + K g'_{m-1} - M f'_{m-1} + M + \lambda^2, \end{aligned} \tag{68}$$

$$R_m^g(\eta) = \Big(1 + \frac{K}{2}\Big) g''_{m-1} + \sum_{k=0}^{m-1} (f_k g'_{m-1-k} - g_k f'_{m-1-k}) - 2K g_{m-1} - K f''_{m-1}, \tag{69}$$

$$\begin{aligned} R_m^\theta(\eta) = {} & \theta''_{m-1} + Pr \sum_{k=0}^{m-1} (f_k \theta'_{m-1-k} - \theta_k f'_{m-1-k} + Ec f''_k f''_{m-1-k}) \\ & - \alpha Pr \theta_{m-1} + Pr Ec f''_{m-1}, \end{aligned} \tag{70}$$

$$\begin{aligned} R_m^h(\eta) = {} & h''_{m-1} + Pr \sum_{k=0}^{m-1} (f_k h'_{m-1-k} - h_k f'_{m-1-k} + Ec f''_k f''_{m-1-k}) \\ & - \alpha Pr h_{m-1} + Pr Ec f''_{m-1}, \end{aligned} \tag{71}$$

$$\chi_m = \begin{cases} 0, & m \leqslant 1, \\ 1, & m > 1. \end{cases} \tag{72}$$

The general solutions to Eqs. (63)–(66) are

$$f_m(\eta) = f_m^*(\eta) + C_1 + C_2 \exp\eta + C_3 \exp(-\eta), \tag{73}$$

$$g_m(\eta) = g_m^*(\eta) + C_4 \exp\eta + C_5 \exp(-\eta), \tag{74}$$

$$\theta_m(\eta) = \theta_m^*(\eta) + C_6 \exp\eta + C_7 \exp(-\eta), \tag{75}$$

$$h_m(\eta) = h_m^*(\eta) + C_8 \exp\eta + C_9 \exp(-\eta), \tag{76}$$

where $f_m^*(\eta)$, $g_m^*(\eta)$, $\theta_m^*(\eta)$, and $h_m^*(\eta)$ are the particular solutions to Eqs. (63)–(66). Note that Eqs. (63)–(66) can be solved by Mathematica one after the other in the order of $m = 1, 2, 3, \cdots$.

3.1 Derivation of coefficients

We will calculate only $A_{m,n}^k$. The rest of all the coefficients can be calculated by the similar procedure. First of all, we calculate the derivatives involving in Eq. (68). From Eqs. (25) and (26), we have

$$\begin{aligned} f'_m(\eta) &= \sum_{n=0}^{2m+1} \Big(\sum_{q=1}^{2m+1-n} q A_{m,n}^q \eta^{q-1} \mathrm{e}^{-n\eta} - \sum_{q=0}^{2m+1-n} n A_{m,n}^q \eta^q \mathrm{e}^{-n\eta} \Big) \\ &= \sum_{n=0}^{2m+1} \Big(\sum_{q=0}^{2m+1-n} (q+1) A_{m,n}^{q+1} \eta^q \mathrm{e}^{-n\eta} - \sum_{q=0}^{2m+1-n} n A_{m,n}^q \eta^q \mathrm{e}^{-n\eta} \Big) \\ &= \sum_{n=0}^{2m+1} \sum_{q=0}^{2m+1-n} ((q+1) A_{m,n}^{q+1} - n A_{m,n}^q) \eta^q \mathrm{e}^{-n\eta} \\ &= \sum_{n=0}^{2m+1} \sum_{q=0}^{2m+1-n} (A_1)_{m,n}^q \eta^q \mathrm{e}^{-n\eta}, \end{aligned} \tag{77}$$

$$\begin{aligned} g'_m(\eta) &= \sum_{n=0}^{2m+1} \Big(\sum_{q=1}^{2m+1-n} q B_{m,n}^q \eta^{q-1} \mathrm{e}^{-n\eta} - \sum_{q=0}^{2m+1-n} n B_{m,n}^q \eta^q \mathrm{e}^{-n\eta} \Big) \\ &= \sum_{n=0}^{2m+1} \Big(\sum_{q=0}^{2m+1-n} (q+1) B_{m,n}^{q+1} \eta^q \mathrm{e}^{-n\eta} - \sum_{q=0}^{2m+1-n} n B_{m,n}^q \eta^q \mathrm{e}^{-n\eta} \Big) \\ &= \sum_{n=0}^{2m+1} \sum_{q=0}^{2m+1-n} ((q+1) B_{m,n}^{q+1} - n B_{m,n}^q) \eta^q \mathrm{e}^{-n\eta} \\ &= \sum_{n=0}^{2m+1} \sum_{q=0}^{2m+1-n} (B_1)_{m,n}^q \eta^q \mathrm{e}^{-n\eta}, \end{aligned} \tag{78}$$

where

$$(A_1)_{m,n}^q = (q+1) A_{m,n}^{q+1} - n A_{m,n}^q, \tag{79}$$

$$(B_1)_{m,n}^q = (q+1) B_{m,n}^{q+1} - n B_{m,n}^q. \tag{80}$$

Similarly,

$$f''_m(\eta) = \sum_{n=0}^{2m+1} \sum_{q=0}^{2m+1-n} (A_2)_{m,n}^q \eta^q \mathrm{e}^{-n\eta}, \tag{81}$$

$$f'''_m(\eta) = \sum_{n=0}^{2m+1} \sum_{q=0}^{2m+1-n} (A_3)_{m,n}^q \eta^q \mathrm{e}^{-n\eta}, \tag{82}$$

$$g''_m(\eta) = \sum_{n=0}^{2m+1} \sum_{q=0}^{2m+1-n} (B_2)_{m,n}^q \eta^q \mathrm{e}^{-n\eta}. \tag{83}$$

Here,

$$(A_2)_{m,n}^q = (q+1)(A_1)_{m,n}^{q+1} - n(A_1)_{m,n}^q, \tag{84}$$

$$(A_3)^q_{m,\,n} = (q+1)(A_2)^{q+1}_{m,\,n} - n(A_2)^q_{m,\,n}, \tag{85}$$

$$(B_2)^q_{m,\,n} = (q+1)(B_1)^{q+1}_{m,\,n} - n(B_1)^q_{m,\,n}. \tag{86}$$

For the product terms, let us consider

$$\begin{aligned}
f_{m-1-k}f''_k &= \sum_{r=0}^{2m-2k-1}\sum_{s=0}^{2m-2k-1-r} A^s_{m-1-k,r}\eta^s \mathrm{e}^{-r\eta} \sum_{i=0}^{2k+1}\sum_{j=0}^{2k+1-i} (A_2)^i_{k,i}\eta^i \mathrm{e}^{i\eta} \\
&= \sum_{r=0}^{2m-2k-1}\sum_{i=0}^{2k+1} \mathrm{e}^{-(r+i)\eta} \sum_{s=0}^{2m-2k-1-r}\sum_{j=0}^{2k+1-i} A^s_{m-1-k,r}(A_2)^i_{k,i}\eta^{j+s} \\
&= \sum_{n=0}^{2m} \mathrm{e}^{-n\eta} \sum_{i=\max\{0,n-2m+2k+1\}}^{\min\{n,2k+1\}} \Big(\sum_{s=0}^{2m-2k-1-r}\sum_{j=0}^{2k+1-i} A^s_{m-1-k,r}(A_2)^j_{k,i}\Big)\eta^{j+s} \\
&= \sum_{n=0}^{2m} \mathrm{e}^{-n\eta} \sum_{i=\max\{0,n-2m+2k+1\}}^{\min\{n,2k+1\}} \Big(\sum_{q=0}^{2m-n} \eta^q \sum_{j=\max\{0,q-2m+2k+1+n-i\}}^{\min\{q,2k+1-i\}} \\
&\quad \cdot A^{q-j}_{m-1-k,n-i}(A_2)^j_{k,i}\Big) \\
&= \sum_{n=0}^{2m}\sum_{q=0}^{2m-n} \Big(\sum_{i=\max\{0,\,n-2m+2k+1\}}^{\min\{n,\,2k+1\}} \sum_{j=\max\{0,\,q-2m+2k+1+n-i\}}^{\min\{q,\,2k+1-i\}} \\
&\quad \cdot A^{q-j}_{m-1-k,\,n-i}(A_2)^j_{k,\,i}\Big)\eta^q \mathrm{e}^{-n\eta},
\end{aligned} \tag{87}$$

$$\begin{aligned}
\sum_{k=0}^{m-1} f_{m-1-k}f''_k = \sum_{n=0}^{2m}\sum_{q=0}^{2m-n} \Big(\sum_{k=0}^{m-1} \sum_{i=\max\{0,\,n-2m+2k+1\}}^{\min\{n,\,2k+1\}} \sum_{j=\max\{0,\,q-2m+2k+1+n-i\}}^{\min\{q,\,2k+1-i\}} \\
\cdot A^{q-j}_{m-1-k,\,n-i}(A_2)^j_{k,\,i}\Big)\eta^q \mathrm{e}^{-n\eta},
\end{aligned} \tag{88}$$

$$\sum_{k=0}^{m-1} f_{m-1-k}f''_k = \sum_{n=0}^{2m}\sum_{q=0}^{2m-n} A^q_{m,\,n}\eta^q \mathrm{e}^{-n\eta}, \tag{89}$$

where

$$A^q_{m,\,n} = \sum_{k=0}^{m-1} \sum_{i=\max\{0,\,n-2m+2k+1\}}^{\min\{n,\,2k+1\}} \sum_{j=\max\{0,\,q-2m+2k+1+n-i\}}^{\min\{q,\,2k+1-i\}} A^{q-j}_{m-1-k,\,n-i}(A_2)^j_{k,\,i}. \tag{90}$$

Similarly, we can calculate the other terms involving in Eq. (68) as follows:

$$\sum_{k=0}^{m-1} f'_{m-1-k}f'_k = \sum_{n=0}^{2m}\sum_{q=0}^{2m-n} (A_1)^q_{m,\,n}\eta^q \mathrm{e}^{-n\eta}, \tag{91}$$

where

$$(A_1)^q_{m,\,n} = \sum_{k=0}^{m-1} \sum_{i=\max\{0,\,n-2m+2k+1\}}^{\min\{n,\,2k+1\}} \sum_{j=\max\{0,\,q-2m+2k+1+n-i\}}^{\min\{q,\,2k+1-i\}} (A_1)^{q-j}_{m-1-k,\,n-i}(A_1)^j_{k,\,i}, \tag{92}$$

$$(A_2)^q_{m,\,n} = \sum_{k=0}^{m-1} \sum_{i=\max\{0,\,n-2m+2k+2\}}^{\min\{n,\,2k+1\}} \sum_{j=\max\{0,\,q-2m+2k+2+n-i\}}^{\min\{q,\,2k+1-i\}} (A_1)^{q-j}_{m-1-k,\,n-i} A^j_{k,\,i}. \tag{93}$$

Using the above relations in Eq. (68), we have

$$h_f R^f_m(\eta) = h_f \sum_{n=0}^{2m-1} \sum_{q=0}^{2m-1-n} ((A_3)^q_{m-1,\,n} - M^2(A_1)^q_{m-1,\,n})\eta^q \mathrm{e}^{-n\eta} + M + \lambda^2$$
$$+ h_f \sum_{n=0}^{2m} \sum_{q=0}^{2m-n} (A^q_{m,\,n} - (A_1)^q_{m,\,n})\eta^q \mathrm{e}^{-n\eta} + h_{\mathrm{f}} \sum_{n=0}^{2m-1} \sum_{q=0}^{2m+1-n} K(B_1)^q_{m,\,n}\eta^q \mathrm{e}^{-n\eta}, \tag{94}$$

$$h_f R^f_m(\eta) = \sum_{n=0}^{2m+1} \sum_{q=0}^{2m+1-n} h_f(\chi_{2m+1-n-q}((A_3)^q_{m-1,\,n} - M^2(A_1)^q_{m-1,\,n})$$
$$+ \chi_{2m+1-n-q}(A^q_{m,\,n} - (A_1)^q_{m,\,n}) + K(B_1)^q_{m,\,n} + M + \lambda^2)\eta^q \mathrm{e}^{-n\eta}, \tag{95}$$

or

$$h_f R^f_m(\eta) = \sum_{n=0}^{2m+1} \sum_{q=0}^{2m+1-n} \Delta^q_{m,\,n}\eta^q \mathrm{e}^{-n\eta}, \tag{96}$$

where

$$\Delta^q_{m,\,n} = h_f(\chi_{2m+1-n-q}((A_3)^q_{m-1,\,n} - M^2(A_1)^q_{m-1,\,n})$$
$$+ \chi_{2m+1-n-q}(A^q_{m,\,n} - (A_1)^q_{m,\,n}) + K(B_1)^q_{m,\,n} + M + \lambda^2). \tag{97}$$

By use of Eq. (96), Eq. (63) becomes

$$L_f(f_m(\eta) - \chi_m f_{m-1}(\eta)) = \sum_{n=0}^{2m+1} \sum_{q=0}^{2m+1-n} \Delta^q_{m,\,n}\eta^q \mathrm{e}^{-n\eta}. \tag{98}$$

Applying the inverse of the linear operator on both sides, we have

$$f_m(\eta) - \chi_m f_{m-1}(\eta) = \sum_{n=0}^{2m+1} \sum_{q=0}^{2m+1-n} \sum_{k=1}^{q+1} \Delta^q_{m,\,n}(\mu_1)^q_{n,\,k}\eta^q \mathrm{e}^{-n\eta} + C^m_1 + C^m_2 \mathrm{e}^{\eta} + C^m_3 \mathrm{e}^{-\eta}, \tag{99}$$

where C_i ($i = 1, 2, 3$) are the constants of the integration. Using boundary conditions, we have

$$C^m_2 = 0, \tag{100}$$

$$C^m_3 = \sum_{q=0}^{2m+1} \Delta^q_{m,\,0}(\mu_1)^q_{0,\,1} + \sum_{q=0}^{2m} \Delta^q_{m,\,1}((\mu_1)^q_{1,\,1} - (\mu_1)^q_{1,\,0})$$
$$+ \sum_{n=2}^{2m+1} \sum_{q=0}^{2m+1-n} \Delta^q_{m,\,n}((\mu_1)^q_{n,\,1} - (\mu_1)^q_{n,\,0}), \tag{101}$$

$$C^m_1 = -\sum_{q=0}^{2m+1} \Delta^q_{m,\,0}(\mu_1)^q_{0,\,1} + \sum_{q=0}^{2m+1} \Delta^q_{m,\,1}(\mu_1)^q_{1,\,1}$$
$$+ \sum_{n=2}^{2m+1} \sum_{q=0}^{2m+1-n} \Delta^q_{m,\,n}(((\mu_1)^q_{n,\,1} - (n-1)(\mu_1)^q_{n,\,0})) \tag{102}$$

with

$$(\mu_1)^q_{n,\,k} = \sum_{r=0}^{q-k} \sum_{p=0}^{q-k-r} \frac{-q!}{k_1(n-1)^{q+1-k-r-p} n^{r+1}(n+1)^{p+1}}. \tag{103}$$

Substituting the values of constants into Eq. (99), we have

$$\begin{aligned}
&\sum_{n=0}^{2m+1} \sum_{q=0}^{2m+1-n} (A^q_{m,\,n} - \chi_{m+2-n}\chi_{m+2-n-q} A^q_{m-1,\,n})\eta^q \mathrm{e}^{-n\eta} \\
&= \sum_{n=0}^{2m+1} \sum_{q=0}^{2m+1-n} \sum_{k=1}^{q+1} \Delta^q_{m,\,n} (\mu_1)^q_{n,\,k} \eta^q \mathrm{e}^{-n\eta} \\
&\quad + \Big(\sum_{q=0}^{2m+1} \Delta^q_{m,\,0} (\mu_1)^q_{0,\,1} + \sum_{q=0}^{2m} \Delta^q_{m,\,1} ((\mu_1)^q_{1,\,1} - (\mu_1)^q_{1,\,0}) \\
&\quad + \sum_{n=2}^{2m+1} \sum_{q=0}^{2m+1-n} \Delta^q_{m,\,n} ((\mu_1)^q_{n,\,1} - (\mu_1)^q_{n,\,0}) \Big) \mathrm{e}^{-\eta} \\
&\quad - \Big(\sum_{q=0}^{2m+1} \Delta^q_{m,\,0} (\mu_1)^q_{0,\,1} - \sum_{q=0}^{2m} \Delta^q_{m,\,1} (\mu_1)^q_{1,\,1} \\
&\quad - \sum_{n=2}^{2m+1} \sum_{q=0}^{2m+1-n} \Delta^q_{m,\,n} ((\mu_1)^q_{n,\,1} - (n-1)\,(\mu_1)^q_{n,\,0}) \Big).
\end{aligned} \tag{104}$$

Comparing like powers of η in the above equations, we arrive at

$$\begin{aligned}
A^0_{m,\,0} &= \chi_m \chi_{m+2} \chi_{m+2-q} A^0_{m-1,\,0} - \sum_{q=0}^{2m} \Delta^q_{m,\,0} (\mu_1)^q_{0,\,1} \\
&\quad - \sum_{n=2}^{2m+1} \sum_{q=0}^{2m+1-n} \Delta^q_{m,\,n} ((\mu_1)^q_{n,\,1} - (n-1)(\mu_1)^q_{n,\,0}),
\end{aligned} \tag{105}$$

$$\begin{aligned}
A^0_{m,\,1} &= \chi_m \chi_{m+1} \chi_{m+1-q} A^0_{m-1,\,0} \\
&\quad - \sum_{q=0}^{2m} \Delta^q_{m,\,1} (\mu_1)^q_{1,\,1} - \sum_{n=2}^{2m+1} \sum_{q=0}^{2m+1-n} \Delta^q_{m,\,n} ((\mu_1)^q_{n,\,1} - n(\mu_1)^q_{n,\,0}),
\end{aligned} \tag{106}$$

$$\begin{aligned}
A^k_{m,\,n} &= \chi_m \chi_{m+2-n} \chi_{m+2-n-q} A^k_{m-1,\,n} - \sum_{q=0}^{m+1-n} \Delta^q_{m,\,n} (\mu_1)^q_{n,\,k} \\
&\quad - \sum_{n=2}^{2m+1} \sum_{q=k}^{2m+1-n} \Delta^q_{m,\,n} ((\mu_1)^q_{n,\,1} - (n-1)(\mu_1)^q_{n,\,0}), \quad n \geqslant 2.
\end{aligned} \tag{107}$$

Using the above recurrence formulas, we can calculate all the coefficient $A^q_{m,\,n}$ by using only

$$A^0_{0,\,0} = R - 1, \quad A^0_{0,\,1} = 1, \quad A^1_{0,\,0} = 1 \tag{108}$$

given by the initial guess approximation in Eq. (25). Our first interest in this section is to ensure the convergence of the series solutions in Eqs. (25)–(28). All these expressions contain the

auxiliary parameter $\hbar$, which plays a vital role in the convergence. Hence, for the determination of an appropriate of $\hbar$, the residual error is computed by the norm 2. The result shows that the minimum residual error locates at $\hbar = -0.25$ (see Fig. 1). Moreover, the displayed $\hbar$-curves in Figs. 2 and 3 with K, M, λ, α, Pr, $R = 1$ and $Ec = 0.5$ find the admissible range of $\hbar$.

The used homotopy-Pade approximations in Tables 1 and 2 accelerate the convergence analysis. Obviously, the values of $\hbar$ depend on the involved physical parameters in the problem.

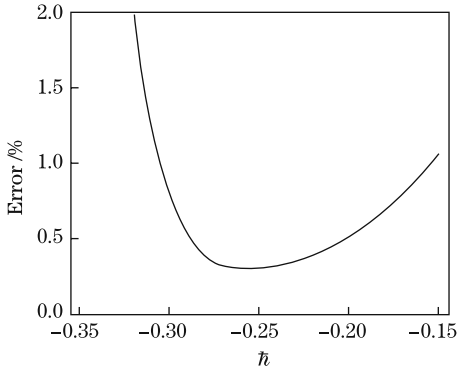

Fig. 1 Residual error of norm 2

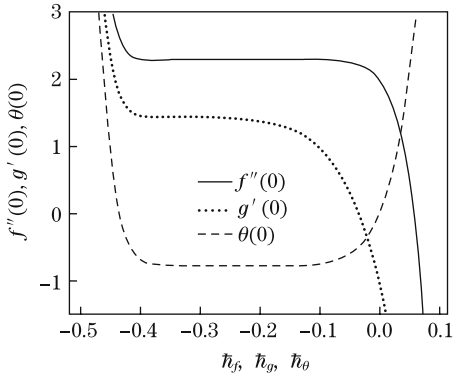

Fig. 2 $\hbar$-curves at 20th-order of approximation for PST case

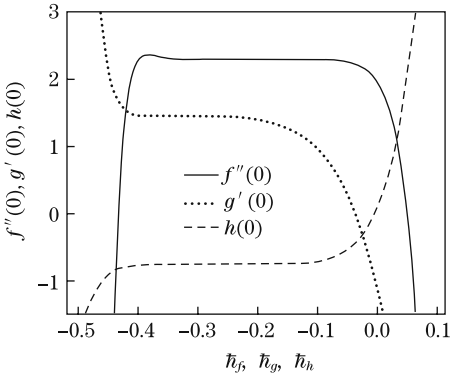

Fig. 3 $\hbar$-curves at 20th-order of approximation for PHF case

Table 1 Convergence of series solutions (PST) by homotopy-Pade approximation

Homotopy-Pade approximation	$-f'(0)$	$-g'(0)$	$-h'(0)$
[2/2]	2.291 49	−0.772 861	1.441 29
[3/3]	2.292 90	−0.772 902	1.453 18
[4/4]	2.293 04	−0.772 166	1.453 21
[5/5]	2.292 96	−0.772 167	1.452 60
[6/6]	2.292 96	−0.772 113	1.446 24
[7/7]	2.292 96	−0.772 114	1.446 23
[8/8]	2.292 96	−0.772 105	1.450 51
[12/12]	2.292 94	−0.772 103	1.450 73
[13/13]	2.292 94	−0.772 103	1.450 75
[14/14]	2.292 94	−0.772 103	1.450 75
[15/15]	2.292 94	−0.772 103	1.450 75

It is observed that the results of the $\hbar$-curves and the homotpy-Pade approximations are in a very good agreement. The coefficient of the skin friction and Nusselt number for different physical parameters and orders of the Pade-approximation are presented in Tables 3 and 4. Clearly, the tabulated values witness the convergence. Moreover, it is noticed that the skin friction coefficient increases when the microrotation parameter K increases. The variations of K on the magnitude of the Nusselt number is qualitively similar to that of the skin friction. In both PST and PHF cases, the skin friction and the Nusselt number have similar observations.

Table 2 Convergence of series solutions (PHF) by homotopy-Pade approximation

Homotopy-Pade approximation	$-f'(0)$	$-g'(0)$	$-h'(0)$
[2/2]	2.291 49	−0.772 861	1.441 29
[3/3]	2.292 90	−0.772 902	1.453 18
[4/4]	2.293 04	−0.772 166	1.453 21
[5/5]	2.292 96	−0.772 167	1.452 60
[6/6]	2.292 96	−0.772 113	1.446 24
[7/7]	2.292 96	−0.772 114	1.446 23
[10/10]	2.292 96	−0.772 105	1.450 51
[12/12]	2.292 94	−0.772 103	1.451 73
[13/13]	2.292 94	−0.772 103	1.451 75
[14/14]	2.292 94	−0.772 103	1.451 75
[15/15]	2.292 94	−0.772 103	1.451 75

Table 3 Values of skin friction and Nusselt number for PST case when $n = 0$

Order of approximations	K, Pr, $\alpha = 1$, $Ec = 0.5$		$K = 2, Pr$, $\alpha = 1, Ec = 0.5$	
	$C_{\mathrm{f}} Re_x^{\frac{1}{2}}$	$Nu_x Re^{-\frac{1}{2}}$	$C_{\mathrm{f}} Re_x^{\frac{1}{2}}$	$Nu_x Re^{-\frac{1}{2}}$
1	5.400 00	−0.933 37	8.100 00	−0.960 86
2	5.715 83	−1.014 32	8.190 83	−1.058 13
3	5.964 34	−1.082 87	8.274 62	−1.144 32
7	6.519 43	−1.141 08	8.487 49	−1.220 63
10	6.682 25	−1.190 41	8.544 51	−1.288 13
13	6.752 07	−1.132 15	8.563 74	−1.347 78
17	6.785 60	−1.132 15	8.570 22	−1.347 78
20	6.793 78	−1.132 15	8.571 20	−1.347 78

Table 4 Values of skin friction and Nusselt number for PHF case when $n = 0$

Order of approximations	K, Pr, $\alpha = 1$, $Ec = 0.5$		$K = 2$, Pr, $\alpha = 1, Ec = 0.5$	
	$C_{\mathrm{f}} Re_x^{\frac{1}{2}}$	$Nu_x Re^{-\frac{1}{2}}$	$C_{\mathrm{f}} Re_x^{\frac{1}{2}}$	$Nu_x Re^{-\frac{1}{2}}$
1	4.000 00	−0.933 37	5.725 00	−0.960 86
2	3.998 75	−1.014 32	5.476 30	−1.058 13
3	3.996 45	−1.082 87	5.251 78	−1.144 32
7	3.980 04	−1.141 08	4.556 26	−1.220 63
10	3.963 55	−1.190 41	4.199 79	−1.288 13
13	3.945 97	−1.132 15	3.943 82	−1.347 78
17	3.923 08	−1.132 15	3.712 44	−1.347 78
20	3.907 27	−1.132 15	3.596 11	−1.347 78

Our second interest in this section is to analyze the influence of the emerging parameters on the velocity, microrotation, and temperature. The results are plotted in Figs. 4–9.

It is observed from Fig. 4 that, with the increase in M, the dimensionless velocity f_η increases and the boundary layer thickness decreases. This leads to a fact that the magnetic field controls

the boundary layer thickness. The similar trend is observed in Fig. 5 for different values of the porosity parameter R on f_η. Figure 6 shows the variations of the microintertia parameter K on the velocity. The velocity field decreases while the layer thickness increases when K increases. Note that these graphs are prepared for strong concentration situations ($n = 0$). It is worth mentioning that the behaviors for the weak concentration ($n = \frac{1}{2}$) are almost similar.

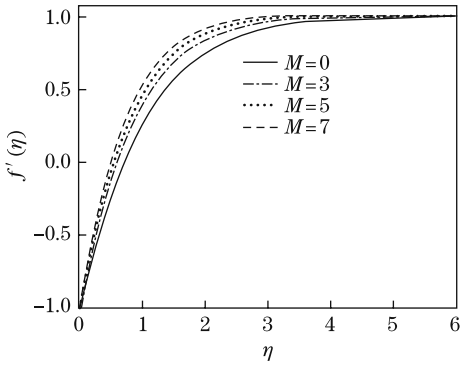

Fig. 4 Velocity profiles for different M with $R, \lambda, K, Pr, \alpha = 1$, $Ec = 0.5$, and $n = 0$

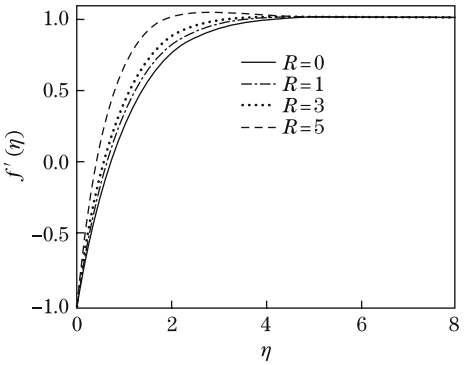

Fig. 5 Velocity profiles for different R with $M, \lambda, K, Pr, \alpha = 1$, $Ec = 0.5$, and $n = 0$

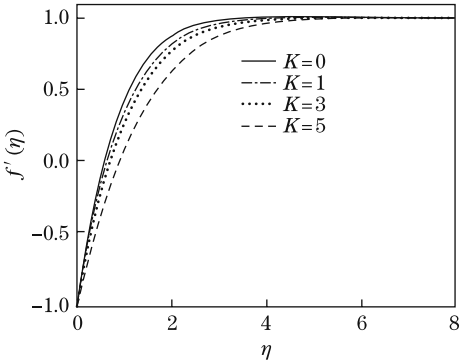

Fig. 6 Velocity profiles for different K with $M, \lambda, R, Pr, \alpha = 1$, $Ec = 0.5$, and $n = 0$

The behaviors of the microrotation g for different M, K, and R are shown in Figs. 7–9. Figure 7 shows that g decreases near the surface while increases away from the surface when M increases. The microrotation g increases with the increase in K, and decreases with the increase in R. However, the layer thickness decreases when both K and R increase (see Figs. 8–9).

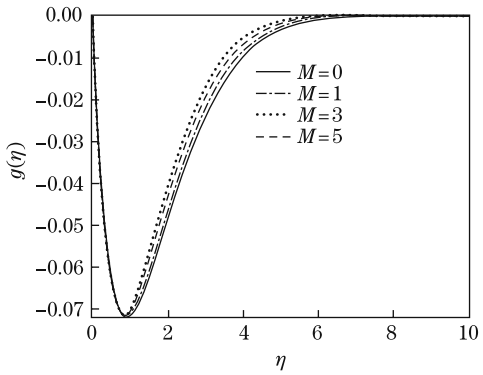

Fig. 7 Velocity profiles for different M with $R, \lambda, K, Pr, \alpha = 1$, $Ec = 0.5$, and $n = 0$

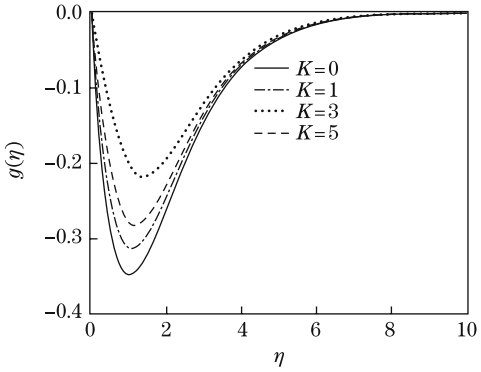

Fig. 8 Velocity profiles for different K with $R, \lambda, M, Pr, \alpha = 1$, $Ec = 0.5$, and $n = 0$

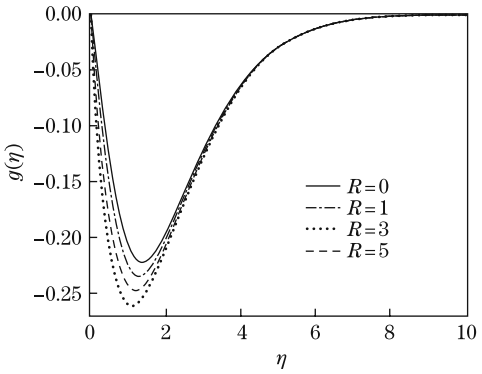

Fig. 9 Velocity profiles for different R with $M, \lambda, K, Pr, \alpha = 1$, $Ec = 0.5$, and $n = 0$

Figures 10–17 indicate the variations of M, K, R, Pr, α, and Ec on the temperature in the PST case. There is a decrease in the temperature when R and M increase, whereas there is an increase when K increases. Near the surface, the temperature increases when Pr increases. This fact is quite different from that when the temperature variation is far away from the surface (see Fig. 15). Figures 13 and 14 depict that the temperature θ increases with the increases

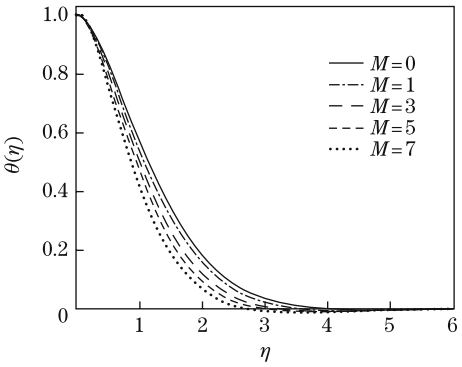

Fig. 10 Temperature profiles (PST) for different M with $R, \lambda, K, Pr, \alpha = 1$, $Ec = 0.5$, and $n = 0$

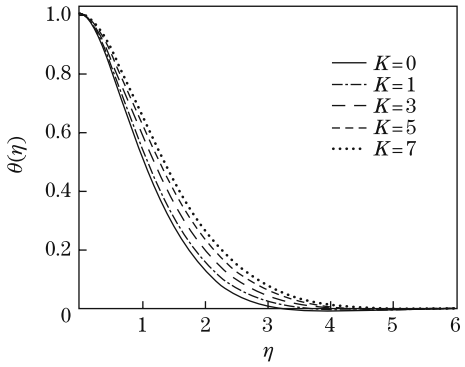

Fig. 11 Temperature profiles (PST) for different K with $R, \lambda, M, Pr, \alpha = 1$, $Ec = 0.5$, and $n = 0$

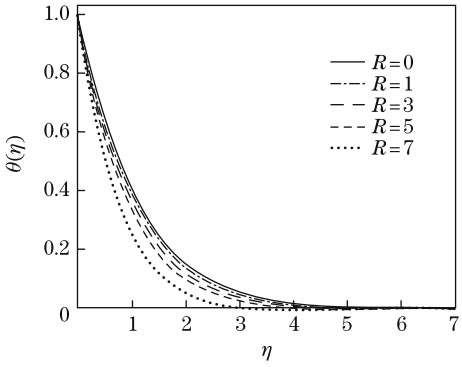

Fig. 12 Temperature profiles (PST) for different R with $M, \lambda, K, Pr, \alpha = 1$, $Ec = 0.5$, and $n = 0$

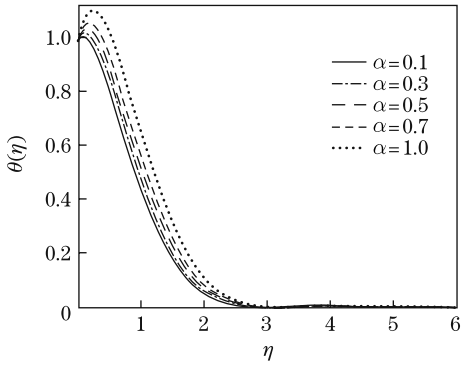

Fig. 13 Temperature profiles (PST) for different α with $M, \lambda, K, Pr, R = 1$, $Ec = 0.5$, and $n = 0$

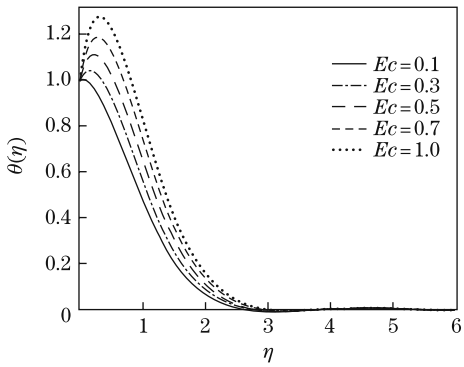

Fig. 14 Temperature profiles (PST) for different Ec with $M, \lambda, K, Pr, R, \alpha = 1$ and $n = 0$

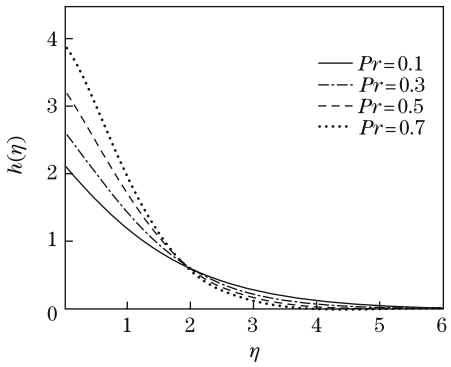

Fig. 15 Temperature profiles (PHF) for different Pr with $M, \lambda, K, \alpha = 1$, $Ec = 0.5$, and $n = 0$

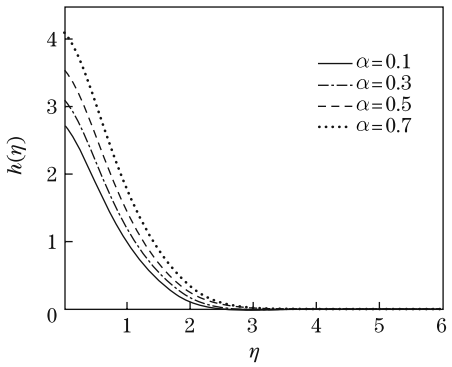

Fig. 16 Temperature profiles (PHF) for different α with $M, \lambda, K, Pr, R = 1$, $Ec = 0.5$, and $n = 0$

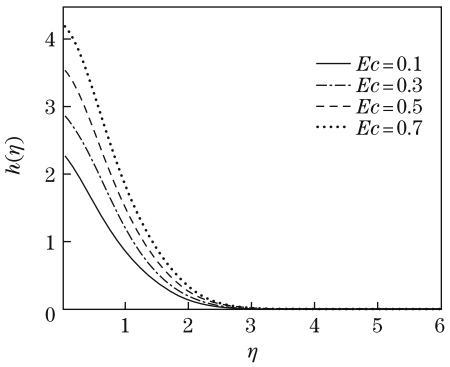

Fig. 17 Temperature profiles (PHF) for different Ec with $M, \lambda, K, Pr, R, \alpha = 1$ and $n = 0$

in α and Ec. Figures 16 and 17 lead to an increase in the temperature $h(\eta)$ when both α and Ec increase. The decrease in the thermal boundary layer is noticed.

4 Conclusions

The present study deals with the MHD stagnation point flow towards a heated shrinking surface subjected to heat generation/absorption. We have the following main observations:

(i) The velocity profile f' increases for negative M. The porosity parameter R and the magnetic parameter M on f' have similar effects in the qualitative sense. However, the material parameter K has opposite effects on f' when compared with M and R.

(ii) The microrotation velocity g increases with the increase in K. Moreover, the roles of M on g are qualitative similar to that of K.

(iii) The variation of the porosity R on the microrotation velocity g is opposite to that of M and K.

(iv) For the PST case, the temperature $\theta(\eta)$ increases with the increases in K, α, and Ec, while decreases with the increases in M and R.

(v) For the PHF case, the temperature $h(\eta)$ increases with the increases in the heat generation parameter α and the Eckert number Ec. However, with the increase in Pr, the temperature first increases, and then decreases.

References

[1] Mahapatra, T. R. and Gupta, A. S. Magnetohydrodynamics stagnation point flow towards a stretching sheet. *Acta Mechanica*, **152**, 191–196 (2001)

[2] Nazar, R., Amin, N., Filip, D., and Pop, I. Unsteady boundary layer flow in the region of the stagnation point on a stretching sheet. *International Journal of Engineering Science*, **42**, 1241–1253 (2004)

[3] Lok, Y. Y., Amin, N., and Pop, I. Unsteady mixed convection flow of a micropolar fluid near the stagnation point on a vertical surface. *International Journal of Thermal Sciences*, **45**, 1149–1157 (2006)

[4] Lok, Y. Y., Amin, N., and Pop, I. Mixed convection flow near a non-orthognal stagnation point towards a stretching vertical plate. *International Journal of Heat and Mass Transfer*, **50**, 4855–4863 (2007)

[5] Wang, C. Y. Off-centered stagnation flow towards a rotating disc. *International Journal of Engineering Science*, **46**, 391–396 (2008)

[6] Xu, H., Liao, S. J., and Pop, I. Series solution of unsteady boundary layer flow of a micropolar fluid near the forward stagnation point of a plane surface. *Acta Mechanica*, **184**, 87–101 (2006)

[7] Nadeem, S., Hussain, M., and Naz, M. MHD stagnation flow of a micropolar fluid through a porous medium. *Meccanica*, **45**, 869–880 (2010)

[8] Kumari, M. and Nath, G. Steady mixed convection stagnation-point flow of upper convected Maxwell fluids with magnetic field. *International Journal of Non-Linear Mechanics*, **44**, 1048–1055 (2009)

[9] Hayat, T., Abbas, Z., and Sajid, M. MHD stagnation-point flow of an upper-convected Maxwell fluid over a stretching surface. *Chaos, Solitons and Fractals*, **39**, 840–848 (2009)

[10] Labropulu, F., Li, D., and Pop, I. Non-orthogonal stagnation-point flow towards a stretching surface in a non-Newtonian fluid with heat transfer. *International Journal of Thermal Sciences*, **49**, 1042–1050 (2010)

[11] Wang, C. Y. and Miklavic, M. Viscous flow due to a shrinking sheet. *Quarterly Applied Mathematics*, **64**, 283–290 (2006)

[12] Fang, T. and Zhong, Y. Viscous flow over a shrinking sheet with an arbitrary surface velocity. *Communications in Nonlinear Science and Numerical Simulation*, **15**, 3768–3776 (2010)

[13] Cortell, R. On a certain boundary value problem arising in shrinking sheet flows. *Applied Mathematics and Computation*, **217**, 4086–4093 (2010)

[14] Nadeem, S. and Awais, M. Thin film flow of an unsteady shrinking sheet through porous medium with variable viscosity. *Physics Letters A*, **372**, 4965–4972 (2008)

[15] Hayat, T., Iram, S., Javed, T., and Asghar, S. Shrinking flow of second grade fluid in a rotating frame: an analytic solution. *Communications in Nonlinear Science and Numerical Simulation*, **15**, 2932–2941 (2010)

[16] Eringen, A. C. Theory of micropolar fluids. *Journal of Mathematics and Mechanics*, **16**, 1–18 (1966)

[17] Eringen, A. C. *Microcontinuum Field Theories*, II: *Fluent Media*, Springer, New York (2001)

[18] Devakar, M. and Iyengar, T. K. V. Stokes' first problem for a micropolar fluid through state-space approach. *Applied Mathematical Modelling*, **33**, 924–936 (2009)

[19] Ali, N. and Hayat, T. Peristaltic flow of a micropolar fluid in an asymmetric channel. *Computers and Mathematics with Applications*, **55**, 589–608 (2008)

[20] Magyari, E. and Kumaran, V. Generalized Crane flows of micropolar fluids. *Communications in Nonlinear Science and Numerical Simulation*, **15**, 3237–3240 (2010)

[21] Ariman, T., Turk, M. A., and Sylvester, N. D. Microcontinuum fluid mechanics — a review. *International Journal of Engineering Science*, **11**, 905–930 (2010)

[22] Hoyt, J. W. and Fabula, A. F. *The Effect of Additives on Fluid Friction*, Defense Technical Information Center, Washington D. C. (1964)

[23] Power, H. Micropolar fluid model for the brain fluid dynamics. *International Conference on Biofluid Mechanics*, New York (1998)

[24] Abbasbandy, S. Homotopy analysis method for the Kawahara equation. *Nonlinear Analysis*: *Real World Applications*, **11**, 307–312 (2010)

[25] Liu, C. S. The essence of the homotopy analysis method. *Applied Mathematics and Computation*, **216**, 1299–1303 (2010)

[26] Liao, S. J. *Beyond Perturbation*: *Introduction to the Homotopy Analysis Method*, Chapman and Hall/CRC Press, Boca Raton (2003)

[27] Liao, S. J. A short review on the homotopy analysis method in fluid mechanics. *Journal of Hydrodynamics*, **22**, 882–884 (2010)

[28] Hayat, T., Naz, R., and Sajid, M. On the homotopy solution for Poiseuille flow of a fourth grade fluid. *Communications in Nonlinear Science and Numerical Simulation*, **15**, 581–589 (2010)

[29] Hayat, T., Qasim, M., and Abbas, Z. Homotopy solution for the unsteady three-dimensional MHD flow and mass transfer in a porous space. *Communications in Nonlinear Science and Numerical Simulation*, **15**, 2375–2387 (2010)

[30] Dinarvand, S., Doosthoseini, A., Doosthoseini, E., and Rashidi, M. M. Series solutions for unsteady laminar MHD flow near forward stagnation point of an impulsively rotating and translating sphere in presence of buoyancy forces. *Nonlinear Analysis*: *Real World Applications*, **11**, 1159–1169 (2010)

[31] Hayat, T. and Javed, T. On analytic solution for generalized three-dimensional MHD flow over a porous stretching sheet. *Physics Letters A*, **370**, 243–250 (2007)

[32] Abbasbandy, S., Yurusoy, M., and Pakdemirli, M. The analysis approach of boundary layer equations of power-law fluids of second grade. *Zeitschrift für Naturforschung*, **63(a)**, 564–570 (2008)

[33] Tan, Y. and Abbasbandy, S. Homotopy analysis method for quadratic Ricati differential equation. *Communications in Nonlinear Science and Numerical Simulation*, **13**, 539–546 (2008)

[34] Hayat, T., Iqbal, Z., Sajid, M., and Vajravelu, K. Heat transfer in pipe flow of a Johnson-Segalman fluid. *International Communications in Heat and Mass Transfer*, **35**, 1297–1301 (2008)

[35] Rees, D. A. S. and Pop, I. Free convection boundary layer flow of a micropolar fluid from a vertical flat plate. *IMA Journal of Applied Mathematics*, **61**, 179–197 (1998)